Neoplasia • Vol. 4, No. 4, 2002, pp. 355–368

www.nature.com/neo

Hepatitis Bx Antigen Stimulates Expression of a Novel Cellular Gene, URG4, that Promotes Hepatocellular Growth and Survival[1]

N. Lale Satiroglu Tufan, Zhaorui Lian*, Jie Liu*, Jingbo Pan*, Patrick Arbuthnot†, Michael Kew†, Marcy M. Clayton*, Minghua Zhu‡ and Mark A. Feitelson*,§*

*Department of Pathology, Anatomy, and Cell Biology, Thomas Jefferson University, Philadelphia, PA, USA; †Molecular Hepatology Research Unit, Department of Medicine, University of the Witwatersrand, Johannesburg, South Africa; ‡Department of Pathology, Second Military Medical College, Shanghai, People's Republic of China; §Department of Microbiology and Immunology, Kimmel Cancer Center, Thomas Jefferson University, Philadelphia, PA, USA

Abstract

Hepatitis B virus encoded X antigen (HBxAg) may contribute to the development of hepatocellular carcinoma (HCC) by up- or downregulating the expression of cellular genes that promote cell growth and survival. To test this hypothesis, HBxAg-positive and -negative HepG2 cells were constructed, and the patterns of cellular gene expression compared by polymerase chain reaction select cDNA subtraction. The full-length clone of one of these upregulated genes (URG), URG4, encoded a protein of about 104 kDa. URG4 was strongly expressed in hepatitis B-infected liver and in HCC cells, where it costained with HBxAg, and was weakly expressed in uninfected liver, suggesting URG4 was an effector of HBxAg *in vivo*. Overexpression of URG4 in HepG2 cells promoted hepatocellular growth and survival in tissue culture and in soft agar, and accelerated tumor development in nude mice. Hence, URG4 may be a natural effector of HBxAg that contributes importantly to multistep hepatocarcinogenesis.

Neoplasia (2002) **4,** 355–368 doi:10.1038/sj.neo.7900241

Keywords: hepatitis B virus, hepatitis Bx antigen, hepatocellular carcinoma, oncogene, pathogenesis.

Introduction

Hepatitis B virus (HBV) is a major etiologic agent associated with chronic liver diseases, such as hepatitis, cirrhosis, and hepatocellular carcinoma (HCC) [1,2]. HCC is among the most common tumor types worldwide, with more than 370,000 cases diagnosed annually, and a survival rate of <3% over 5 years [2,3]. The relative risk of HBV carriers developing HCC is in excess of 100, suggesting that the relationship between HBV and HCC is one of tightest between a virus and a human cancer [2,4].

The molecular mechanisms underlying this high risk for tumor development are incompletely understood, although the chronic carrier state and the progression of chronic liver disease are major risk factors [1–5]. HBV also encodes a protein known as hepatitis Bx antigen (HBxAg) that appears to participate in the development of HCC [6,7]. For example, the X gene of HBV is commonly integrated into host DNA at many, apparently random sites [8]. Many of these integration events result in the generation of X region mRNA [9,10] and HBxAg [11–14] in infected liver and tumor. HBxAg also directly correlates with the severity of liver disease [15]. In some strains of X transgenic mice with sustained high levels of HBxAg, HCC develops [16,17]. X region DNA from the virus genome and from HCC nodules have been shown to transform a liver cell line [18,19]. These independent lines of evidence suggest that HBxAg contributes importantly to hepatocarcinogenesis.

HBxAg is a *trans*-activating protein [20], and it has been proposed that the effects of HBxAg on the transcription of cellular genes underlies the mechanism whereby HBV contributes to the high risk of HCC [6,7]. Interestingly, HBxAg *trans*-activation appears to be carried out through the stimulation of multiple cytoplasmic signal transduction pathways, such as those involving ras [21], nuclear factor kappa B (NF-κB) [22], activating protein-1 (AP-1) [23], and janus kinase (JAK)/signal transducer and activator of transcription (STAT) [24]. In the nucleus, HBxAg *trans*-activation appears to involve the binding of HBxAg to a variety of transcription factors, such as a subunit of RNA polymerase II [25], TATA binding protein [26], activating transcription factor-2 [27], and other components of the basal transcriptional machinery [28,29]. HBxAg also binds to an ultraviolet-induced DNA binding protein involved in DNA repair [30], and disrupts p53/excision-repair cross-complementing type 3 protein complexes [31], which may disrupt transcription coupled repair, suggesting that HBxAg may promote the accumulation of mutations. In addition, HBxAg binds to and inactivates the

Abbreviations: CAT, chloramphenicol acetyltransferase; FCS, fetal calf serum; G3PDH, glyceraldyde-3-phosphate dehydrogenase; HBV, hepatitis B virus; HBxAg, hepatitis Bx antigen; HCC, hepatocellular carcinoma; IGF, insulin-like growth factor; ISH, *in situ* hybridization; MTT, modified tetrazolium salt assay; PCR, polymerase chain reaction; URG4, upregulated geneclone 4

Address all correspondence to: Dr. Mark Feitelson, Room 222, Alumni Hall, Department of Pathology, Anatomy, and Cell Biology, Thomas Jefferson University, 1020 Locust Street, Philadelphia, PA 19107-6799, USA. E-mail: mark.feitelson@mail.tju.edu

[1]This work was supported by NIH grants CA48656 and CA66971 to M.F. Tufan, Lian, and Liu contributed equally to this study.

Received 5 December 2001; Accepted 24 January 2002.

negative growth regulators p53 [31,32] and $p55^{sen}$ [33], as well as decrease the expression of the cyclin-dependent kinase inhibitor $p21^{WAF1/CIP1/SDI1}$ [34] and the translation initiation factor sui1 [35], both of which also negatively regulate cell growth. Hence, there are multiple pathways whereby HBxAg may alter cellular gene expression. It is likely that these alterations contribute importantly to hepatocarcinogenesis, because HBxAg regulates apoptosis [36-38], mediates resistance to anti–Fas killing [39], stimulates cell cycle [40], and promotes survival in serum-free medium [39].

With few exceptions, the natural effectors of HBxAg that promote tumor development have not been identified or well characterized. For example, HBxAg appears to upregulate the expression of insulin-like growth factor 2 (IGF-2) and the IGF-1 receptor in HCC [41,42]. Given that the IGF-1 receptor binds to both IGF-1 and -2, it is possible that HBxAg may set up an autocrine loop that enhances cell growth. HBxAg also reportedly *trans*-activates c-*jun*, alphafetoprotein, and the pancreatic secretory trypsin inhibitor in reporter gene assays [43,44], but it is not known whether these events occur *in vivo*. To systematically identify natural effectors of HBxAg, experiments were designed to test the hypothesis that the introduction of HBxAg into HepG2 cells is associated with the altered expression of selected cellular proteins. This work identifies and characterizes one of the HBxAg upregulated genes (URG), referred to as URG4, which accelerates cell growth and promotes tumor formation.

Materials and Methods

Cell Lines and Tissue Culture Conditions

The human hepatoblastoma cell line, HepG2 [45] (ATCC, Manassas, VA), was cultured on type-1 rat tail collagen (Becton Dickinson, Franklin Lakes, NJ)-coated tissue culture dishes or plates. Cells were grown in Earle's modified Eagle's medium supplemented with 10% heat-inactivated fetal calf serum (FCS), 100 μM minimal essential medium non–essential amino acids, 1 mM sodium pyruvate, as well as standard concentrations of penicillin plus streptomycin.

HepG2.2.2.15 cells (a kind gift from Dr. George Acs, Mount Sinai School of Medicine), which support HBV replication [46], and the retrovirus packaging cell line, PA317 [47], were also grown in the same conditions.

Plasmids

The retroviral plasmid, pSLXCMVneo, was used to clone the HBV X gene or the bacterial chloramphenicol acetyltransferase (CAT) gene sequences, exactly as described [33,48]. To verify correct cloning, DNA samples were prepared by using Wizard Plus Minipreps DNA Purification Systems (Promega, Madison, WI) and then sequenced in the DNA sequencing facility at the Kimmel Cancer Institute of Thomas Jefferson University.

pcDNA3 (Invitrogen, SanDiego, CA) was used to clone full-length upregulated gene, clone 4 (URG4) cDNA under the control of the immediate early CMV promoter and also used for the cloning of the HBx open reading frame, as described [35].

Establishment of HBxAg-Positive and -Negative HepG2 Cells

Recombinant retroviruses encoding HBx (from pSLX-CMV–HBx) or CAT (from pSLXCMV–CAT) were prepared [49], titered, and then used to transduce separate cultures of HepG2 cells, as described [48]. Cultures were then selected in G418 for 14 days to maximize the fraction of cells producing HBxAg or CAT. Standard CAT assays were performed on HepG2CAT lysates using ^{14}C-chloramphenicol, and acetylated forms were separated by thin-layer chromatography [35,48]. Lysates prepared from 5×10^6 HepG2X cells were assayed for HBxAg by Western blotting with a mixture of HBx peptide antibodies using previous published procedures [35,48].

Polymerase Chain Reaction (PCR) Select cDNA Subtraction, Cloning, Sequencing, and Identification of a cDNA from a Putative HBxAg Effector

The differences in gene expression, which distinguish HepG2X from HepG2CAT cells, were determined by using a commercially available subtraction hybridization approach (the PCR-select cDNA subtraction kit from Clontech, Palo Alto, CA) according to the instructions provided by the manufacturer, with minor modifications [48]. The PCR fragments corresponding to differentially expressed mRNA were cloned, sequenced, and compared to existing sequences in GenBank. One of these differentially expressed PCR fragments, initially designated as URG4, was chosen for further characterization.

Cloning and Sequencing the Full-Length URG4 cDNA

The full-length cDNA clone containing the URG4 sequences was obtained by the rapid amplification of 5′ and 3′ cDNA ends PCR method using the Marathon cDNA Amplification Kit (Clontech) as described [48]. Briefly, one 3′ and one 5′ gene specific primers were synthesized. By using these gene-specific primers together with an adaptor primer, PCR was performed with human placental cDNA as template to get the 3′ or 5′ cDNA-specific products in separate amplification reactions. The products were cloned into pT7Blue(R) T vector (Novagen, Madison, WI) and sequenced. The appropriate 3′ and 5′ gene-specific fragments were then digested with *Not*I and *Bcl*I restriction enzymes and cloned into pcDNA3 (Invitrogen) at the chosen sites. The integrity of the full-length clone was verified by DNA sequencing. The full-length sequence was compared to those for homology to known genes in NCBI–GenBank using the nucleotide Basic Local Alignment Search Tool.

Preparation and Use of URG4 Antisera

The full-length cDNA from URG4 was used to deduce the corresponding amino acid sequence using the TRANSLATE program. Hydrophilic and potentially antigenic peptides were deduced from the PEPTIDESTRUCTURE and PLOTSTRUCTURE programs [50] and made by solid phase

peptide synthesis in the Peptide Synthesis Facility on campus. Two peptides, which span inclusive residues 460–483 (24 amino acids) and 821–838 (18 amino acids), were coupled to keyhole limpet hemocyanin carrier and used to raise antisera in New Zealand rabbits (two rabbits/peptide), as described [51]. Antisera were initially characterized by specific enzyme-linked immunosorbent assays. For Western blotting, each antiserum was used at a dilution of 1:1000, and blotting was conducted by using a mixture of antisera from both specificities. Western blots for β-actin were performed as an internal (sample loading) control using commercially available antibody (Ab-1; Oncogene Research Products, Cambridge, MA), as described [35]. Horseradish peroxidase-conjugated goat anti–rabbit Ig (Accurate, Westbury, NY) and ECL substrate (Amersham, Arlington Heights, IL) were used for detection.

Immunohistochemical staining was performed on slides prepared from formalin-fixed, paraffin-embedded tissues using the Vectastain Elits avidin–biotin-complex Kit according to manufacturer's instructions (Vector laboratories, Burlingame, CA) with minor modifications [14]. A mixture of rabbit antibodies raised against URG4 (each at 1:4000 dilution) or HBxAg (used at a dilution of 1:8000) synthetic peptides were used as primary antibodies. Biotinylated anti–rabbit Ig was used as secondary antibody, and diaminobenzidine was used as substrate for detection. Preimmune serum or preincubation of primary antibodies with an excess of the corresponding synthetic peptide(s) (25 μg of each peptide for 1 hour at 37°C) served as controls. For HBxAg staining, uninfected liver was used as an additional control. Immunohistochemistry was evaluated independently by two pathologists counting stained and total hepatocytes in five random fields per slide by light microscopy at a magnification of $\times$200.

Construction of URG4-Overexpressing HepG2 and Control Cells

To study the properties of URG4 compared to HBxAg on the cellular level, separate cultures of 1×10^6 HepG2 cells were stably transfected with 10 μg of pcDNA3, pcDNA3–URG4, or pcDNA3–HBx using SuperFect transfection reagent (QIAGEN, Valencia, CA) according to the instructions provided by the manufacturer. Cells were selected with G418 (800 μg/ml) for 4 weeks. URG4 and HBx mRNA expression was assayed by Northern blotting, whereas protein expression was characterized by immunostaining or Western blotting [35,48].

RNA Isolation and Northern Blot Analysis of URG4

Total RNA was isolated from HepG2X, HepG2CAT, HepG2.2.15, HepG2–pcDNA3, or HepG2–pcDNA3–URG4 cells using Tri-Reagent (Molecular Research Center, Cincinnati, OH). Extracted RNA was precipitated with isopropanol, and then assessed for integrity of ribosomal RNA by agarose gel electrophoresis. RNA samples were then blotted onto nylon membranes (Hybond-N, Amersham). Northern blotting was carried out using the URG4 probe obtained from cDNA subtraction that had been labeled by random priming (Amersham). Following autoradiographic exposure, membranes were stripped and rehybridized with a radiolabeled glyceraldehyde-3-phosphate dehydrogenase (G3PDH) probe (Clontech). The G3PDH signal served to normalize the URG4 mRNA levels following gel scanning.

Patient Samples

Paired tumor and nontumor liver tissues used for analysis were obtained from 23 Chinese and 14 South African patients chronically infected with HBV who had undergone surgery for the removal of their tumors. Additional characteristics of these patients were previously published [35,48]. Analogous pieces of uninfected human liver from five Chinese individuals, who were seronegative for HBV, were available to serve as controls. In addition, paired tumor/nontumor from lung, breast, thyroid, spleen, stomach, pancreas, kidney, and sigmoid colon were obtained from patients who had undergone surgery for the removal of their tumors at Thomas Jefferson University Hospital. Formalin-fixed, paraffin-embedded tissues were collected from most patients, used for diagnostic purposes, and were then made available for these studies. Use of all tissues for this work was approved by the Institutional Review Board at Thomas Jefferson University.

In Situ Hybridization (ISH)

The URG4 cDNA fragment obtained from PCR select cDNA subtraction was used as a probe for ISH to validate the RNA subtraction procedure in HepG2X compared to HepG2CAT cells, and to detect URG4 mRNA in tumor, infected liver, and uninfected tissues. ISH was carried out using the Oncor ISH and digoxigenin/biotin detection kits according to the instructions provided by the manufacturer (Oncor, Gaithersburg, MD). Criteria used for evaluation were the same as that outlined above for immunohistochemical staining.

Growth of HepG2–pcDNA3, –pcDNA3–HBx, or –pcDNA3–URG4 Cells in Complete or Serum-Free Medium

HepG2 cells stably transfected with pcDNA3, pcDNA3–HBx, or pcDNA3–URG4 were seeded into six-well plates in duplicate and grown in complete or serum-free medium. The number of viable cells was determined at daily intervals after seeding for up to 5 days by trypan blue staining. Cell viability was independently determined using the modified tetrazolium salt (MTT) assay, as described by the manufacturer (Cell Titer 96 Non–Radioactive Cell Proliferation Assay, Promega). Results represent three independent experiments, each done in duplicate.

Flow Cytometry

To asses the effect of URG4 on cell growth, 1×10^5 HepG2 cells stably transfected with pcDNA3, pcDNA3–HBx, or pcDNA3–URG4 were seeded into 60-mm plates and incubated overnight in complete medium. Cells were synchronized in serum-free medium for 48 hours, then

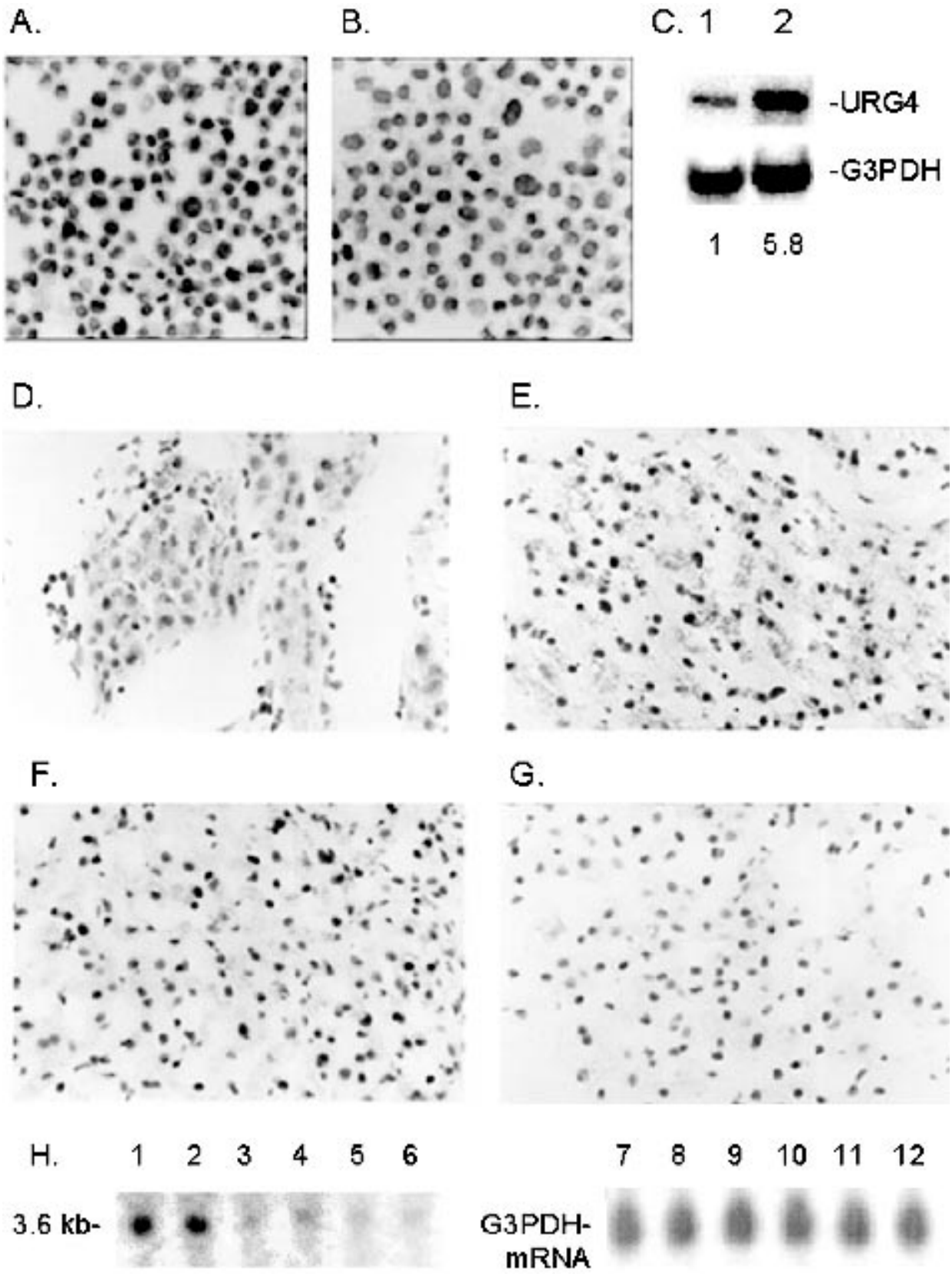

Figure 1. *Differential expression of URG4 mRNA in HepG2X compared to HepG2CAT cells by ISH and Northern blot analysis. ISH was performed on HepG2X cells (A) and HepG2CAT cells (B) using the cDNA fragment of URG4 obtained from cDNA subtraction as probe (original magnification, ×20). Northern blot analysis of RNA extracted from HepG2CAT (panel C, lane 1) and HepG2X (panel C, lane 2) cells using the URG4 probe, and after stripping the membrane, with the G3PDH probe. The normalized average ratio of URG4 mRNA in HepG2CAT:HepG2X cells is indicated below the blot. ISH was also performed on fresh frozen sections of HCC (D), nontumor liver from a carrier (E), and uninfected liver (F). In panel G, the tissue in panel C was hybridized with an irrelevant probe. (H) Northern blot analysis of URG4 mRNA from nontumor samples of two patients (lanes 1 and 2), from tumor samples of two patients (lanes 3 and 4), and from two uninfected liver samples (lanes 5 and 6). The G3PDH controls for lanes 1–6 are in lanes 7–12.*

incubated in 10% FCS containing medium, fixed, stained with propidium iodine, and analyzed by the Flow Cytometry Facility at Thomas Jefferson University at 24 and 48 hours time points.

Growth of URG4-Overexpressing Cells in Soft Agar and in Nude Mice

HepG2–pcDNA3, HepG2–pcDNA3–HBx, and HepG2–pcDNA3–URG4 were tested for anchorage-independent growth in soft agar and for tumor formation in nude mice. For growth in soft agar, 1×10^4 cells/well were seeded in triplicate into six-well plates, and allowed to grow for 21 days. The colonies were then counted under code. For tumorigenicity assays, 1×10^7 viable cells (by trypan blue exclusion) were injected subcutaneously at a single site in nude mice. The mice were observed over 6 weeks for tumor formation. The mice were then sacrificed and the tumors recovered for further analysis. The use of mice for this work was reviewed and approved by the Institutional Animal Care and Use Committee at Thomas Jefferson University.

Statistical Analysis

The relationship between ISH and protein staining results for URG4, and between URG4 and HBxAg staining, have been evaluated in 2×2 tables in a two-tailed analysis. The results were significant when $P<.05$. The mean difference in growth between HepG2 cell stably transfected with pcDNA3, pcDNA3–HBx, or pcDNA3–URG4 was analyzed using the Student's *t* test. A significant difference was recognized when $P<.05$.

Results

PCR Select cDNA Subtraction and Identification of URG4

It has been proposed that HBxAg *trans*-activating properties contribute to the altered patterns of host gene expression that is important for the development of HCC [7]. To test this hypothesis, HepG2 cells were transduced with recombinant retroviruses encoding HBxAg or the bacterial CAT gene. When RNA from these two cultures were compared by PCR select cDNA subtraction, eight up- and two downregulated genes were observed. One of these upregulated genes, URG4, consisted of a cDNA fragment of ~1.7 kb in length that was 99% homologous to an uncharacterized segment in the short arm of chromosome 7.

Before characterizing this gene product in detail, this cDNA fragment was used as a probe for ISH and for Northern blot analysis to verify that the subtractive hybridization worked. When this probe was used for ISH on HepG2X cells, the great majority of the cells showed a dark cytoplasmic brown staining (Figure 1*A*). In contrast, ISH on HepG2CAT cells showed faint or no staining (Figure 1*B*). ISH with an irrelevant probe [pT7Blue(R) T] failed to hybridize to either HepG2X or HepG2CAT cells (data not shown). To quantitate the differences in URG4 mRNA levels in HepG2X compared to HepG2CAT cells, the 1.7-kb URG4 cDNA fragment was used as a probe in Northern blot analysis. A G3PDH probe, which detected an RNA at about 1.3 kb, was used for normalization. The URG4 probe detected a single band of about 3.6 kb in size that is expressed 5.8±0.3 times higher in HepG2X compared to HepG2CAT cells (Figure 1*C*). These combined results verify that the PCR select cDNA subtraction procedure yielded a cDNA fragment that was upregulated in HepG2X compared to HepG2CAT cells.

Expression of URG4 in Tumor, Nontumor, and Uninfected Liver

If URG4 is an effector of HBxAg that is important for tumor development, then its expression should be upregulated in the livers and/or tumors of HBV carriers compared to liver tissues from uninfected individuals. To test this hypothesis, ISH was performed in tumor and surrounding nontumor liver, as well as in tissues from five uninfected individuals. The URG4 cDNA probe yielded easily detectable signals in tumor cells (Figure 1*D*) from 8 of 14 South African patients (57%) and from 11 of 23 Chinese patients (48%) (Table 1), suggesting that URG4 was expressed in HCC. In nontumor tissue, the URG4 probe also yielded widespread and strong signals (Figure 1*E*) in 13 of 14 South African patients (93%) and in 21 of 23 Chinese patients (91%) (Table 1). In contrast, faint ISH signals were observed in three of the five livers from uninfected individuals (60%) (Figure 1*F*, Table 1). ISH of nontumor liver tissue from the same patient in Figure 1*E* with an irrelevant probe [pT7Blue(R) T vector] yielded no detectable signal (Figure 1*G*), underscoring the specificity of the method. Since the hybridization signals in nontumor liver tissue from many patients in both populations appeared to be more intense than the signals observed in the corresponding tumor cells from the same patients, a more quantitative measure of these differences was obtained by Northern blotting. In samples where intact RNA was obtained, Northern blot analysis showed a single band at about 3.6 kb in extracts from both tumor and nontumor tissue, although the levels in nontumor tissue (Figure 1*H*, *lanes* 1 and 2) were up to several fold higher than in corresponding tumor tissue (Figure 1*H*, *lanes* 3 and 4) from the same patients. This RNA is the same size as that

Table 1. Summary of ISH Results for the URG4 Probe in Tumor/Nontumor Pairs for HCC Patients from South Africa and China.

South African Patients															Uninfected Livers				
Case No.:	1	2	3	4	5	6	7	8	9	10	11	12	13	14	1	2	3	4	5
tumor	0	1	0	0	1	2	4	1	1	0	1	0	0	1					
nontumor	4	2	2	2	3	4	4	2	2	3	4	0	1	2	1	1	0	1	0

Chinese Patients																									
Case No.:	1	2	3	4	5	6	7	8	9	10	11	12	13	14	15	16	17	18	19	20	21	22	23
tumor	1	0	1	0	1	1	0	1	0	0	0	1	2	1	0	1	0	0	1	0	0	0	1
nontumor	1	2	1	1	2	1	0	2	1	1	1	2	1	2	2	2	1	0	2	2	3	4	2

ISH staining is estimated as follows: 0: no signal; 1: ISH signal in <10% of cells; 2: ISH signal in 10–25% of cells; 3: ISH signal in 25–50% of cells; 4: ISH signal in >50% of cells. T: tumor; NT: nontumor.

observed in HepG2 cells (Figure 1*C*). In contrast, lower levels of hybridization were observed in uninfected liver tissues (Figure 1*H*, *lanes* 5 and 6), suggesting that the expression of URG4 is higher in infected compared to uninfected tissue, and that it is generally higher in nontumor compared to tumor cells.

Cloning of Full-Length URG4 and Characterization of URG4 Protein Expression

Based on the results of ISH, full-length URG4 cDNA was obtained by rapid amplification of 5′ and 3′ cDNA ends, and the full-length cDNA then cloned into pcDNA3. Sequence analysis of URG4 cDNA showed a short 5′ untranslated region of 13 bases, followed by an open reading frame of 2766 bases that encodes a polypeptide 922 amino acids long with a calculated molecular weight of 103,876 Da (Figure 2). The 3′ untranslated region consists of 828 bases, which adds up to 3.607 kb for the full-length URG4 mRNA. This is approximately the size of the RNA detected by Northern blotting in HepG2 cells (Figure 1*C*) and in liver (Figure 1*H*). The URG4 polypeptide did not have any identifiable motifs suggesting function, save the existence of a possible ATP/GTP binding site motif spanning amino acids 690–697. Functional analysis failed to show that URG4 bound to or hydrolyzed any of the nucleoside triphosphates, suggesting that this putative binding site motif is not active (data not shown). When the full-length URG4 sequence was analyzed by the basic local alignment search tool to find

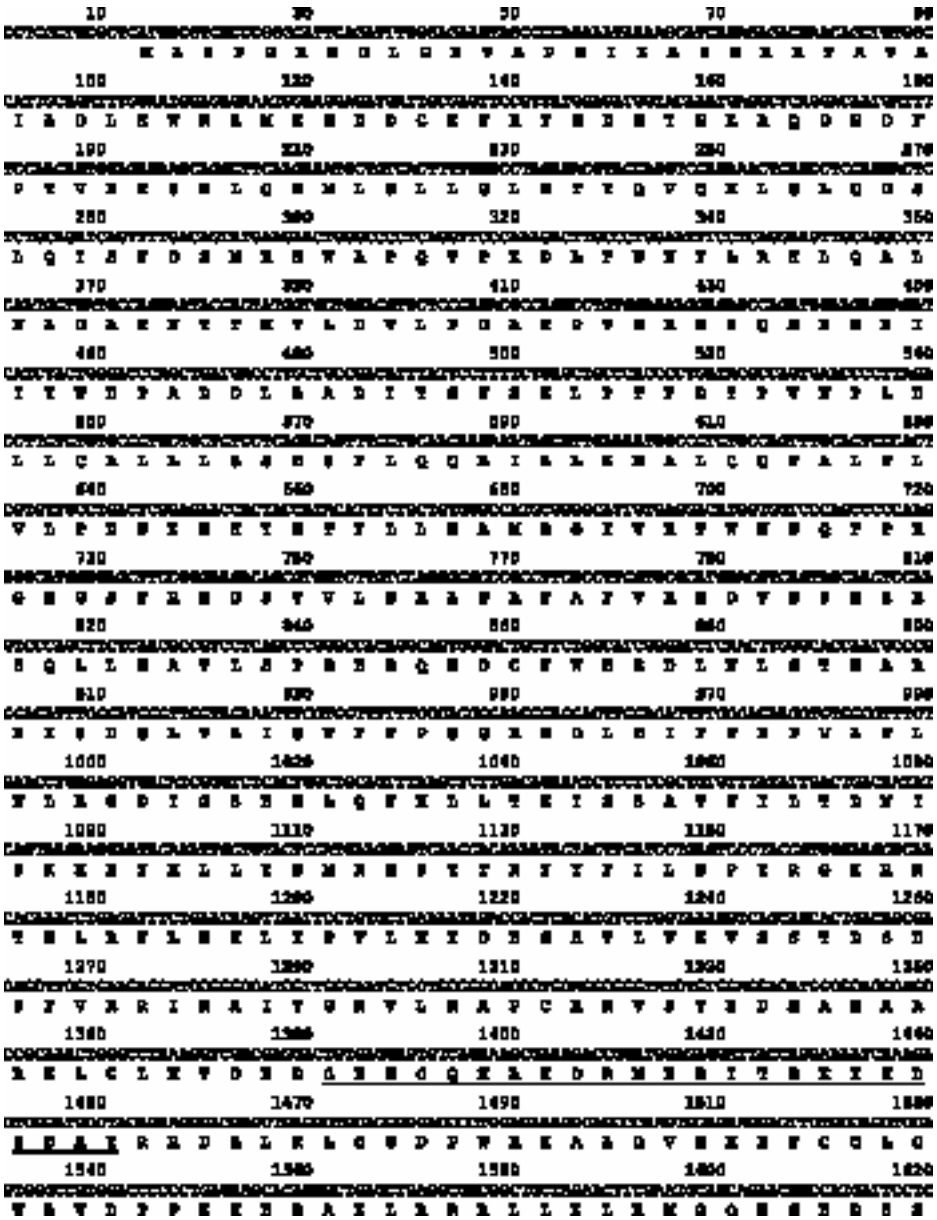

Figure 2. *Nucleic acid and protein sequence of full-length URG4. The putative adenosine triphosphate/guanosine triphosphate binding site spans amino acids 690–697 (corresponding to nts 2081–2102) and is bold, italicized, and underlined. The synthetic peptides made to raise corresponding antisera are underlined. Peptide A spans amino acid residues 457–480 (24 amino acids) (corresponding to nts 1382–1451) and peptide B spans amino acid residues 817–834 (18 amino acids) (corresponding to nts 2462–2513).*

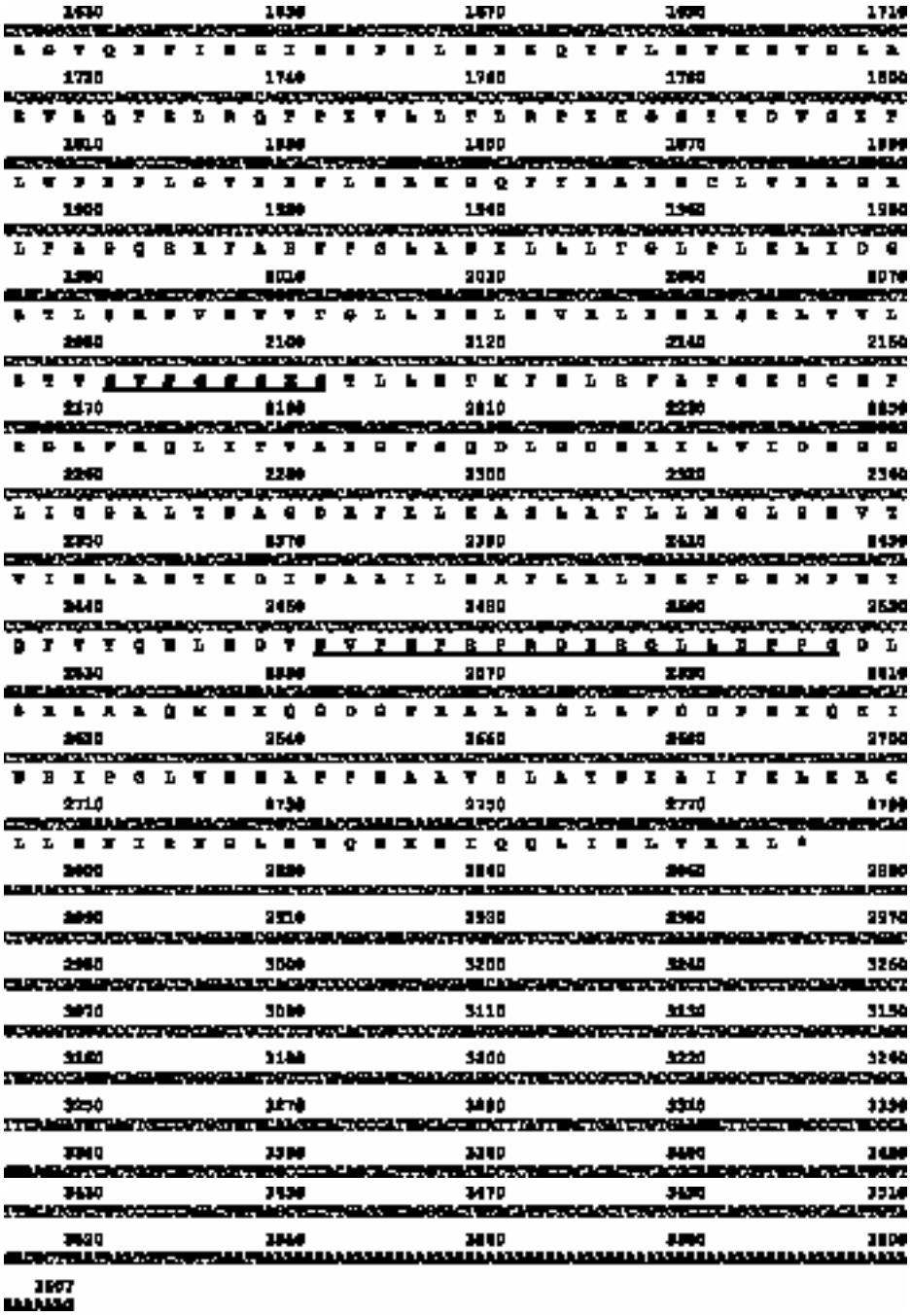

Figure 2. (*continued*)

homology with known genes, the search again failed to identify URG4 with any previously published sequence.

To determine the patterns of URG4 protein distribution, selected synthetic peptides were made (Figure 2) and used to generate corresponding antibodies in rabbits. Immunohistochemical staining was then carried out with formalin-fixed, paraffin-embedded tissue samples from South African and Chinese carriers. Among South African patients, staining was observed with anti-URG4 in tumor tissue from 8 of 14 patients (57%), whereas staining was observed in 11 of 23 tumor samples from Chinese patients (48%) (Table 2). In surrounding nontumor liver tissue, staining with anti-URG4 was observed in 13 of 14 South African patients (93%) and in 21 of 23 Chinese patients (91%) (Table 2). Staining was exclusively cytoplasmic in tumor and nontumor liver cells from both sets of patients (Figure 3). When URG4 ISH and immunohistochemical results were compared in tumor for both groups of patients, a strong positive correlation was observed ($P < .001$). Similar results were obtained when these features were compared in nontumor liver from both groups ($P < .001$), suggesting upregulation of both RNA and protein in the same patients. When staining was conducted in consecutive sections of tumor from individual patients, there was clear colocalization of URG4

Table 2. Summary of Immunohistochemistry (IHC) for the URG4 and HBxAg in Tumor/Nontumor Pairs for HCC Patients from South Africa and China.

South African Patients															Uninfected Livers				
Case No.:	1	2	3	4	5	6	7	8	9	10	11	12	13	14	1	2	3	4	5
T: URG4	0	1	0	1	1	0	3	1	1	0	2	0	0	1					
HBxAg	0	1	0	2	2	0	3	0	1	0	1	0	0	0					
NT: URG4	3	2	2	1	3	2	4	3	1	2	3	0	2	3	1	1	0	1	0
HBxAg	1	2	1	3	3	0	4	1	1	2	2	0	0	1	0	0	0	0	0

Chinese Patients																							
Case No.:	1	2	3	4	5	6	7	8	9	10	11	12	13	14	15	16	17	18	19	20	21	22	23
T: URG4	2	0	1	0	1	1	0	2	0	0	0	1	1	2	0	1	0	0	1	0	0	0	2
HBxAg	1	0	0	1	0	1	0	2	1	0	1	0	0	1	0	2	0	0	0	0	0	2	2
NT: URG4	2	1	2	2	2	1	0	3	2	1	2	1	1	2	2	3	1	0	2	1	2	4	3
HBxAg	3	1	1	2	1	2	1	3	1	0	2	1	1	1	2	3	2	0	1	2	1	2	2

Staining is estimated as follows: 0: no signal; 1: IHC signal in <10% of cells; 2: IHC signal in 10–25% of cells; 3: IHC signal in 25–50% of cells; 4: IHC signal in >50% of cells. T: tumor; NT: nontumor.

(Figure 3*A*) and HBxAg (Figure 3*B*). Preimmune rabbit serum derived from animals that were subsequently immunized with the URG4 synthetic peptides showed no staining on consecutive tissue sections (Figure 3*C*). Identical results were obtained with preimmune serum from rabbits that were later immunized with HBxAg polypeptides (data not shown, but exactly like Figure 3*C*). Analogous results were obtained when staining was performed in infected nontumor liver tissue using anti-URG4 (Figure 3*D*), anti-HBx (Figure 3*E*), or preimmune serum (Figure 3*F*). Statistical analysis independently confirmed the close association between URG4 and HBxAg in nontumor liver ($P<.005$). When sections from uninfected liver were evaluated, weak staining was observed in the same three of five samples (Figure 3*G*) that also had detectable ISH signals (Tables 1 and 2). Pretreatment of primary antibodies with an excess of the corresponding synthetic peptides eliminated staining (data not shown). These results suggest colocalization of URG4 and HBxAg in HCC and surrounding nontumor liver from HBV-infected patients, and that the expression of URG4 was apparently upregulated in infected tissue.

To further explore the tissue distribution of URG4, anti-URG4 was used to stain samples from pancreas, lung, breast, thyroid, spleen, stomach, kidney, and sigmoid colon tissue sections from uninfected patients. Staining was observed in the cytoplasm of up to 10% of ductal epithelial cells from the pancreas (data not shown). None of the other uninfected tissues examined had positive staining. URG4 staining was also observed in the tumor cells from a case of poorly differentiated pancreatic cancer, but was absent from tumor samples of the lung (non–small cell lung cancer), thyroid (follicular adenoma), breast (invasive intraductal cancer), sigmoid colon (moderately differentiated adenocarcinoma), and kidney (papillary transition cell carcinoma) (data not shown). In all cases, the results were based on staining a single normal or tumor specimen of each tissue type. These results suggest a restricted tissue and tumor-type distribution of URG4 expression.

Construction and Growth of HepG2 Cells Stably Transfected with pcDNA3–HBx, pcDNA–URG4, or pcDNA3

To functionally characterize URG4, independent cultures of HepG2 cells were stably transfected with pcDNA3, pcDNA3–HBx, or pcDNA3–URG4, and each of the cell lines selected in G418. The levels of URG4 mRNA and protein were then determined in each of the cell lines by Northern and Western blotting, respectively. Parallel analyses were done with HepG2.2.15 cells to assess URG4 levels in the context of virus replication. Northern blot analysis (Figure 4*A*) showed a single band of 3.6 kb in HepG2–pcDNA3 cells (lane 1), whereas the levels were 2.8±0.3-fold higher in HepG2–pcDNA3–HBx cells (lane 2), and 5.1±0.7-fold higher in HepG2 cells stably transfected with pcDNA3–URG4 (lane 3). For comparison, the levels of URG4 mRNA in HepG2.2.15 cells was 2.3±0.23 higher than in HepG2–pcDNA3 (lane 4). Interestingly, the levels of URG4 mRNA correlated with the levels of HBxAg polypeptide, both of which were roughly two-fold higher in HepG2 cells transduced with recombinant retrovirus encoding HBxAg compared to HepG2 cells stably transfected with pcDNA3–HBx, suggesting dose dependence (data not shown). When Western blotting was conducted with lysates prepared from the cell lines in panel 4A, a major immunoreactive band at about 105 kDa was expressed in HepG2–pcDNA3 cells (Figure 4*B*, lane 1), at 2.3±0.5-fold higher levels in HepG2–pcDNA3–HBx cells (lane 2), and at 5.5±0.6-fold higher levels in HepG2 cells overexpressing URG4 (lane 3). ^{35}S–URG4 prepared by *in vitro* translation was included for comparison (lane 4). In HepG2.2.15 cells, URG4 was also detected at 2.4±0.28-fold higher than control cells (lane 5). The finding that endogenous URG4 polypeptide comigrates with the *in vitro* translation product, and that its size based on sodium dodecyl sulfate/polyacrylamide gel electrophoresis is similar to the calculated value for this protein (103,876 Da), suggests that this band is full-length URG4. These results also verify the expression of URG4 at different levels in these cell lines.

Experiments were then designed to ask whether URG4 overexpression altered cell growth and survival. When these cell lines were grown in tissue culture medium containing 10% FCS (Figure 4*C*) or in serum-free medium (Figure 4*D*), HepG2–pcDNA3–HBx cells grew faster than HepG2–pcDNA3 cells. Statistical analysis showed a significant difference in medium containing 10% FCS on days 2 ($P=.027$), 3 ($P=.01$), 4 ($P=.006$), and 5 ($P=.002$), and in serum-free medium on days 2 ($P=.008$), 3 ($P=.025$), 4 ($P=.004$), and 5 ($P=.002$). HepG2 cells that overexpressed URG4 also significantly stimulated the growth in medium containing 10% FCS on days 2 ($P=.033$), 3 ($P=.022$), 4 ($P=.012$), and 5 ($P=.005$) compared to HepG2–pcDNA3 controls. HepG2.2.15 cells, which also had elevated URG4 (Figure 4*B*), grew significantly faster than control cells on days 2–5 ($.02<P<.03$), although slower than HepG2–pcDNA3 and HepG2–pcDNA3–HBx on days 4 and 5 (Figure 4*C*). When HepG2–pcDNA3–URG4 cells were

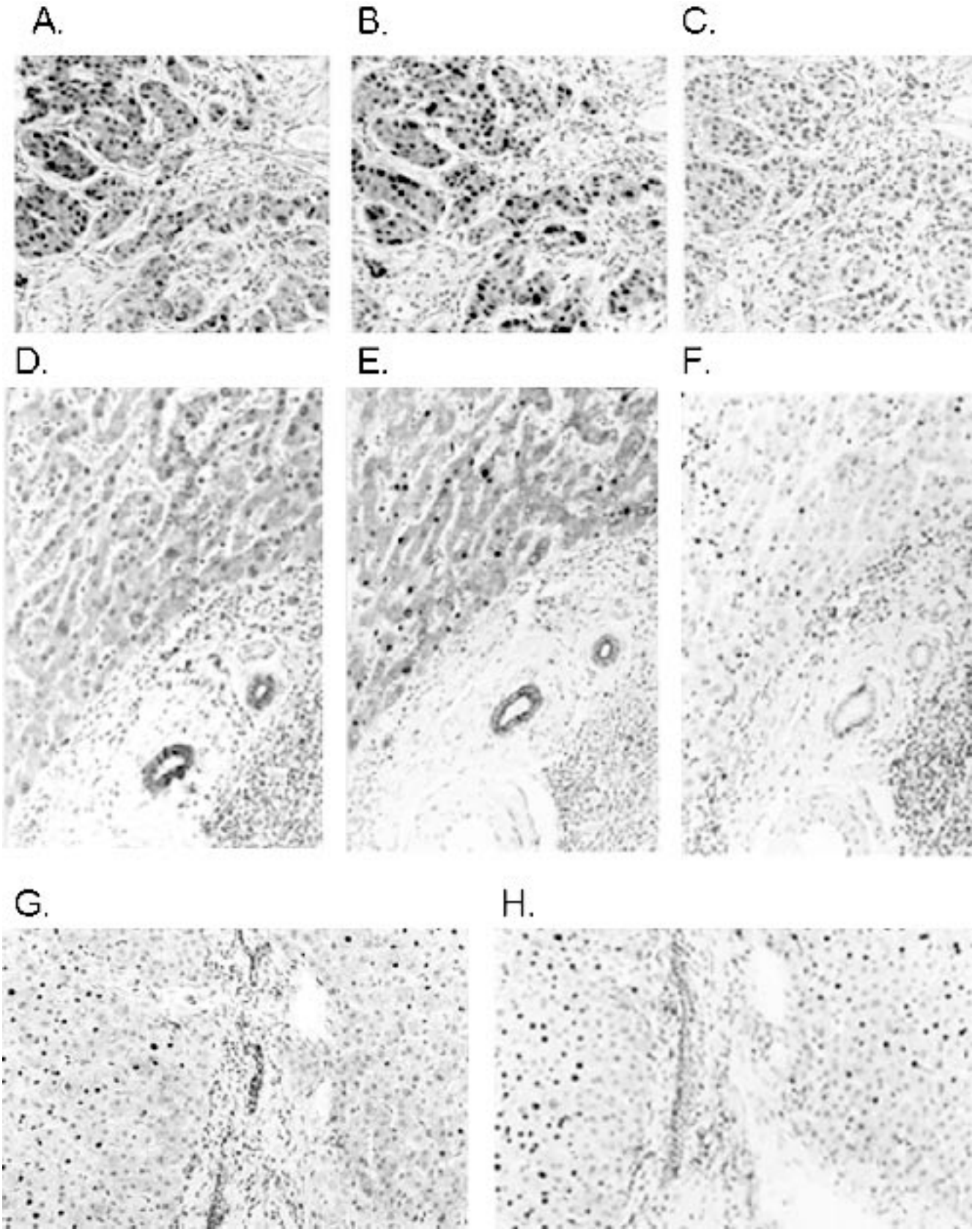

Figure 3. *Immunohistochemical staining for URG4 and HBxAg. (A) Anti-URG4 staining of HCC tissue from an HBV carrier. (B) Anti-HBx staining of a consecutive section from the same patient as in panel A. (C) Preimmune rabbit serum used to stain a consecutive section from the same patient as in panel A. (D) Anti-URG4 staining of nontumor liver tissue from an HBV carrier. (E) Anti-HBx staining of a consecutive section from the same patient as in panel D. (F) Preimmune rabbit serum used to stain a consecutive section from the same patient as in panel D. (G) Anti-URG4 used to stain an uninfected liver. (H) Preimmune rabbit serum used to stain a consecutive section of the same uninfected liver. Original magnification in all panels, ×200.*

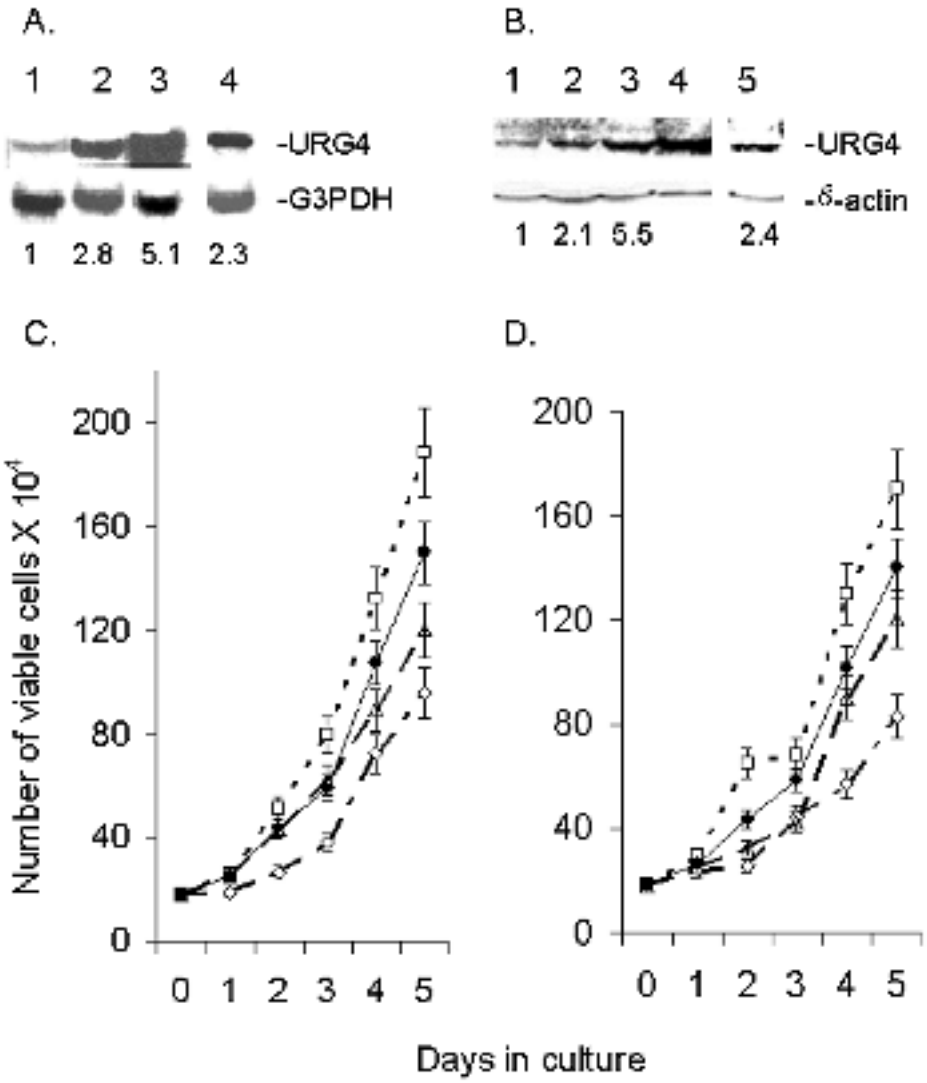

Figure 4. *URG4 expression and growth of HepG2–pcDNA3, HepG2–pcDNA3–HBx, and HepG2–pcDNA3–URG4. (A) Northern blot analysis was carried out on RNA isolated from HepG2–pcDNA3 (lane 1), HepG2–pcDNA3–HBx (lane 2), HepG2–pcDNA3–URG4 cells (lane 3), and HepG2.2.15 (lane 4). Hybridization was carried out with URG4 or G3PDH probes. The numbers below the lanes are the relative amounts of URG4 mRNA in the Northern blot based on gel scanning and corrected by comparison with the corresponding G3PDH control shown below each lane. (B) Western blotting with anti-URG4 was conducted on protein isolated from HepG2–pcDNA3 (lane 1), HepG2–pcDNA3–HBx (lane 2), HepG2–pcDNA3–URG4 (lane 3), and HepG2.2.15 (lane 5). A pcDNA3–URG4 in vitro translation sample (lane 4) was used as a positive control. The numbers below the lanes are the relative amounts of URG4 protein in the Western blot on gel scanning and normalized by comparison with the corresponding β-actin loading control shown below each sample. (C and D) Growth curves for HepG2–pcDNA3 (✧), pcDNA3–HBx (□), pcDNA3–URG4 (●), or HepG2.2.15 (△) cells in complete medium containing 10% FCS (C) or in serum-free medium (D). The curves represent the average of three independent experiments, each done in duplicate.*

grown in serum-free medium, significant growth stimulation was observed at days 4 (P=.003) and 5 (P=.002) compared to HepG2–pcDNA3 cells (Figure 4*D*). URG4 also stimulated growth on days 2 (P=.041) and 3 (P=.046) compared to control cells, although these increases were near the limits of statistical significance. These results suggest that URG4 independently stimulates hepatocellular growth in the absence of HBxAg. However, URG4 overexpression did not stimulate the growth of HepG2 cells as much as HBxAg. Statistical analysis showed the differences in this comparison to be of borderline significance (Figure 4C). To confirm whether URG4 stimulates cell growth, these cell lines were analyzed by flow cytometry following synchronization in serum-free medium. At 24 hours after the addition of 10% FCS to synchronized cells, 25.8% of HepG2–pcDNA3 cells were in S phase, whereas 38.5% of HepG2–pcDNA3–URG4-overexpressing cells were in S phase, and the percentage for HepG2–pcDNA3–HBx cells was 45.1% (Figure 5). Again, the difference between control cells and URG4-overexpressing cells was statistically significant (P=.006), as was the relationship between control and HepG2–pcDNA3–HBx cells (P=.002). At 48 hours, there was no difference in the percentage of cells in each culture that were in S phase, and the values ranged from 21% to 25% of cells in S phase. A larger percentage of HepG2.2.15 cells were in S phase compared to HepG2–pcDNA3 cells, although this was less than that observed for HepG2–pcDNA3–URG4 cells and HepG2–pcDNA3–HBx (data not shown). Hence, URG4 stimulates cell growth in culture and promotes the entry of cells into S phase.

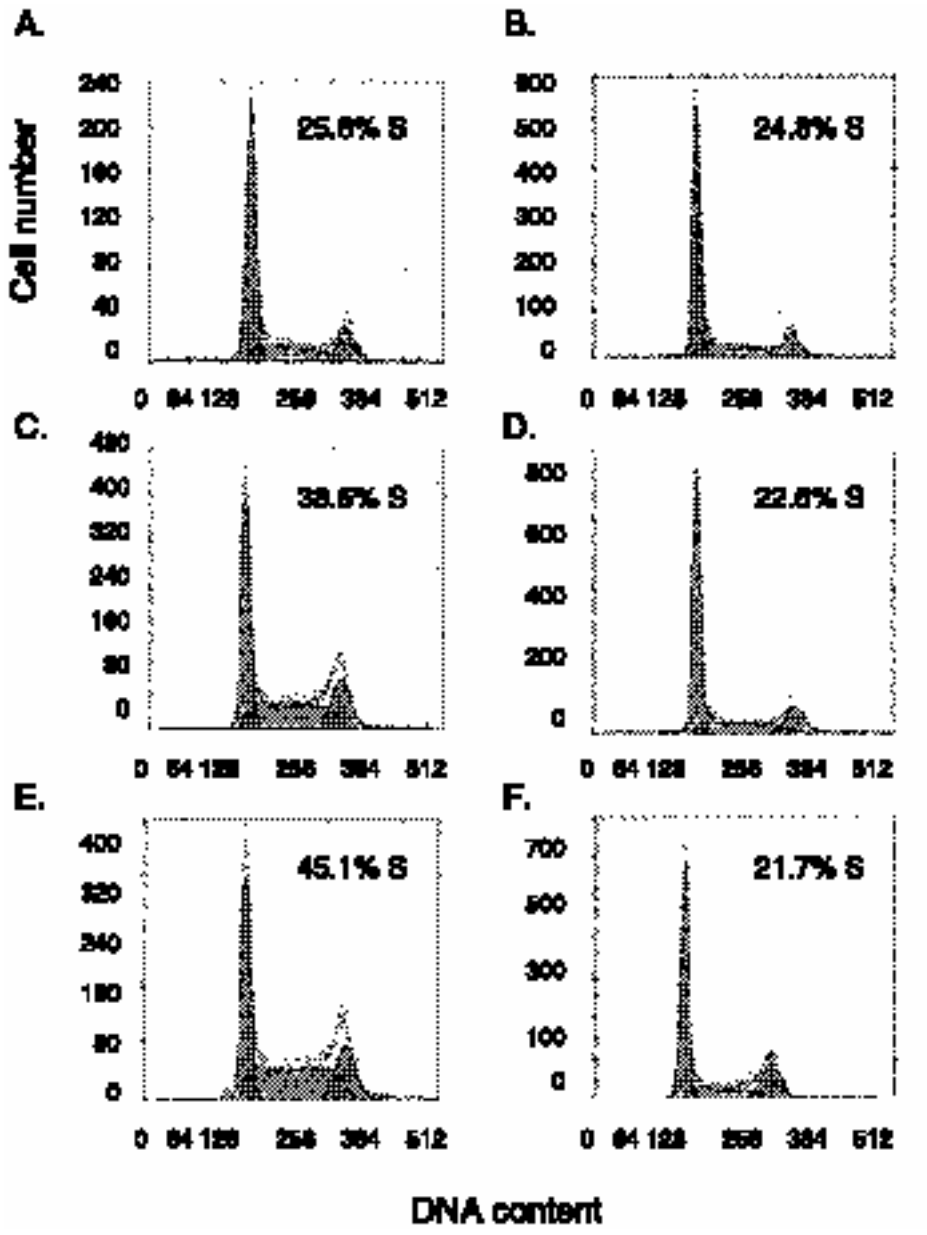

Figure 5. *Flow cytometry of HepG2–pcDNA3 (panels A and B), HepG2–pcDNA3–URG4 (panels C and D), and HepG2–pcDNA3–HBx (panels E and F) cells at 24 hours (panels A, C, and E) and 48 hours (panels B, D, and F) after synchronization and addition of 10% FCS. The results shown here illustrate one of the three independent analyses each done in duplicate.*

Growth in Soft Agar and Tumor Formation

The URG4-mediated stimulation of HepG2 growth in culture prompted the design of additional experiments to test whether this growth stimulation extended to anchorage independence and tumor formation. When these cell lines were seeded into soft agar, HepG2–pcDNA3–HBx cells yielded an average of 44±8 colonies, whereas HepG2–pcDNA3 control cells yielded 10±3 colonies after 21 days ($P<.005$) (Table 3). In comparison, HepG2–pcDNA3–URG4 cells yielded 24±4 colonies, which was significantly higher than control cells ($P<.01$), but not statistically different than HBxAg-producing cells ($P>.1$) (Table 3). Together, these results suggest that URG4 stimulates growth in soft agar, although not as strongly as HBxAg. When these cell lines were individually injected subcutaneously into the backs of nude mice, the majority of mice developed tumors, but the tumors formed by injection of

Table 3. Growth of URG4-Overexpressing HepG2 Cells in Soft Agar.

Experiment	No. of Colonies		
	HepG2–vector	HepG2–URG4	HepG2–HBx
1	7±2	20±3	34±6
2	11±3	24±3	47±8
3	12±4	28±5	50±9

Each experiment was done in triplicate.

Table 4. Tumor Formation with Subcutaneous Injection of HepG2 Cells Stably Transfected with pcDNA3 or pcDNA3–URG4 in Nude Mice.

Cell Line	No. of Mice	No. (%) of Mice with Tumors	Tumor Onset (day)*	Average Tumor Size (cm^3)†
HepG2–pcDNA3	20	15 (75)	43	0.94±0.34
pcDNA3–URG4	10	10 (100)	23	1.96±0.54
pcDNA–HBx	10	7 (70)	36	1.95±0.51

*The day of onset is the first day when a palpable tumor could be detected.†The average size of tumor was determined on day 50 after the injection of tumor cells.

HepG2–pcDNA3–URG4 became palpable by 23±3 days postinjection compared to control cells, which became palpable by 43±5 days postinjection ($P<.005$) (Table 4). The tumors also grew to an average of twice the size in mice injected with HepG2–pcDNA3–URG4 compared to control cells, although these differences did not reach statistical significance ($P>.4$) (Table 4). Interestingly, HepG2–pcDNA3–HBx cells also yielded accelerated tumor growth, and larger tumor size compared to control cells, although only tumor onset was statistically significant ($P<.02$) (Table 4). These results demonstrate that URG4 promotes tumor cell growth *in vivo*.

Discussion

The alteration of host gene expression by HBxAg may be important for the pathogenesis of chronic liver disease and the development of HCC, by activating several signal transduction pathways and affecting the activation of selected transcription factors that regulate proliferation, differentiation, transformation, and invasive growth [5,7]. In this work, experiments were designed to test the hypothesis that introduction of HBxAg into HepG2 cells is associated with altered patterns of host cell gene expression that regulate cell growth and survival. This report describes the isolation and partial characterization of a novel gene, URG4, which is upregulated in the presence of HBxAg, and may contribute importantly to the development of HCC by promoting hepatocellular growth and survival.

Based on PCR select cDNA subtraction of RNA obtained from HBxAg-positive and -negative cell lines, a cDNA fragment, designated URG4, appeared to be expressed at higher levels in HBxAg-positive compared to negative cells. This was confirmed by ISH using the cells from each of these lines (Figure 1, *A* and *B*) and quantitated by Northern blotting (Figures 1*C* and 4*A*) as well as Western blotting (Figure 4*B*). These findings validate the subtraction methodology used and show that URG4 is upregulated at the RNA and protein levels in the presence of HBxAg. To determine whether URG4 was upregulated in HBV infected compared to uninfected liver, ISH was performed on fresh frozen sections from HCC, nontumor liver, and uninfected liver samples. Strong hybridization signals were detected in nontumor liver samples from HBV-infected patients with HCC, at lower levels in the tumor cells from some of the same patients, and at still lower levels in uninfected liver tissue (Figure 1, *D–G*). Again, these results were confirmed and quantitated by Northern blot analysis (Figure 1*H*), and suggest that URG4 was differentially expressed at the RNA level in infected compared to uninfected liver tissue. At the protein level, immunohistochemical staining was noticeably stronger among infected tumor and nontumor specimens compared to uninfected liver (Figure 3) suggesting again that URG4 expression is upregulated in infected compared to uninfected liver. The fact that HBxAg staining strongly correlated with that of URG4 (Figure 3) in many patients from two geographically disperse populations, not only suggests that URG4 upregulated expression occurs commonly in the liver and tumor of carriers with HCC, but also that URG4 is likely to be a natural effector of HBxAg *in vivo*. This is further strengthened by the observation that URG4 polypeptide was upregulated in HBxAg-positive cells, and in cells replicating HBV compared to HBxAg-negative control cells (Figure 4*B*).

HBxAg stimulates cell growth and survival in a number of published reports [5,16-18,40,48], and such a property is likely to contribute importantly to the development of HCC. Hence, if URG4 is a natural effector of HBxAg in chronic infection, it should have at least some of the functions associated with HBxAg. For example, the finding that HBxAg stimulates growth in medium containing 10% serum as well as in serum-free medium, and that URG4 also stimulates growth and survival under these conditions (Figure 4, *C* and *D*), is consistent with the hypothesis that URG4 is an effector of HBxAg that carries out, at least in part, an HBxAg-associated activity that may contribute to the development of HCC. The fact that URG4 overexpression only partially stimulates cell growth and survival under these conditions is consistent with the probability that other HBxAg effectors, such as the recently published URG7 [48], may also contribute importantly to hepatocellular growth and survival. In this context, it will be important to determine whether the URG4 stimulation of cell growth and survival is associated with the constitutive activation of one or more signal transduction pathways that are known to be activated by HBxAg and that are associated with the HBxAg-mediated stimulation of cell growth [7,21,40]. HBx stimulates cell cycle progression by shortening the emergence of cells from quiescence (G_0) and entry into S phase and also accelerating transit through checkpoint controls at G_0/G_1 and G_2/M [40]. The data from flow cytometry with URG4-overexpressing cells (Figure 5) is consistent with this possibility. In addition, by disturbing the regulation of the checkpoint controls, HBx (through URG4?) may contribute to genetic instability, in which unrepaired transforming mutations would accumulate during the pathogenesis of HCC [40].

HBxAg is also known to transform cells *in vitro* [18] and give rise to HCC in selected strains of X transgenic mice

characterized by sustained, high levels of HBxAg expression [16,17]. To test whether URG4 contributes to hepatocarcinogenesis, URG4-overexpressing cells were seeded into soft agar, and tested for anchorage-independent growth, which is an important, although not invariable feature of the transformed cell phenotype. The finding that oncogenes often stimulate anchorage-independent growth when introduced into cells [52,53], and that URG4 stimulates anchorage-independent growth in soft agar (Table 3), suggests that URG4 may be an oncogene operative in hepatocarcinogenesis. This is further supported by the finding that URG4 stimulates tumor formation in nude mice (Table 4).

In summary, HBxAg stimulates the expression of an oncogene in preneoplastic liver that promotes growth factor-independent survival, anchorage-independent growth, and accelerates tumor formation. Given that this upregulation occurs in many patients from two different parts of the world further suggests that URG4 is a natural effector of HBxAg that contributes frequently and importantly to the mechanism of HBxAg-mediated hepatocellular transformation.

References

[1] Arbuthnot P, and Kew M (2001). Hepatitis B virus and hepatocellular carcinoma. *Int J Exp Pathol* **82**, 77–100.

[2] Beasley RP, and Hwang LY (1984). Epidemiology of hepatocellular carcinoma. In *Viral Hepatitis and Liver Disease*. GN Vyas, JL Dienstag and JH Hoofnagle (Eds). Grune and Stratton, New York. pp. 209–24.

[3] Parkin DM, Pisani P, and Ferlay J (1999). Estimation of the worldwide incidence of twenty-five major cancers. *Int J Cancer* **80**, 827–41.

[4] Beasley RP (1988). Hepatitis B virus. The major etiology of hepatocellular carcinoma. *Cancer* **61**, 1942–56.

[5] Feitelson MA, and Duan LX (1997). Hepatitis B virus X antigen in the pathogenesis of chronic infections and the development of hepatocellular carcinoma. *Am J Pathol* **150**, 1141–57.

[6] Caselmann WH (1995). Transactivation of cellular gene expression by hepatitis B viral proteins: a possible molecular mechanism of hepatocarcinogenesis. *J Hepatol* **22(1 Suppl)**, 34–37.

[7] Henkler F, and Koshy R (1996). Hepatitis B virus transcriptional activators: mechanisms and possible role in oncogenesis. *J Viral Hepatol* **3**, 109–21.

[8] Matsubara K, and Tokino T (1990). Integration of hepatitis B virus DNA and its implications for hepatocarcinogenesis. *Mol Biol Med* **7**, 243–60.

[9] Diamantis ID, McGandy CE, Chen TJ, Liaw YF, Gudat F, and Bianchi L (1992). Hepatitis B X gene expression in hepatocellular carcinoma. *J Hepatol* **15**, 400–403.

[10] Paterlini P, Poussin K, Kew M, Franco D, and Brechot C (1995). Selective accumulation of the X transcript of hepatitis B virus in patients negative for hepatitis B surface antigen with hepatocellular carcinoma. *Hepatology* **21**, 313–21.

[11] Katayama K, Hayashi N, Sasaki Y, Kasahara A, Ueda K, Fusamoto H, Sato N, Chisaka O, Matsubara K, and Kamada T (1989). Detection of hepatitis B virus X gene protein and antibody in type B chronic liver disease. *Gastroenterology* **97**, 990–98.

[12] Vitvitski L, Meyers ML, Sninsky JJ, Berthillon P, Chevalier P, Sells MA, Acs G, and Trepo C (1988). Expression of the X gene product of hepatitis B virus and WHV in infected livers and transfected 3T3 cells: evidence for cross-reactivity and correlation with core/e gene expression. In *Viral Hepatitis and Liver Disease.* AJ Zuckerman (Ed). Alan R. Liss, New York. pp. 341–44.

[13] Wang W, London WT, and Feitelson MA (1991). Hepatitis B x antigen in hepatitis B virus carrier patients with liver cancer. *Cancer Res* **51**, 4971–77.

[14] Wang W, London WT, Lega L, and Feitelson MA (1991). Hepatitis B x antigen in liver from carrier patients with chronic hepatitis and cirrhosis. *Hepatology* **14**, 29–37.

[15] Feitelson MA, Lega L, Duan LX, and Clayton M (1993). Characteristics of woodchuck hepatitis X antigen in the livers and sera from chronically infected animals. *J Hepatol* **17(Suppl 3)**, S24–34.

[16] Koike K, Moriya K, Iino S, Yotsuyanagi H, Endo Y, Miyamura T, and Kurokawa K (1994). High-level expression of hepatitis B virus HBx gene and hepatocarcinogenesis in transgenic mice. *Hepatology* **19**, 810–19.

[17] Ueda H, Ullrich SJ, Gangemi JD, Kappel CA, Ngo L, Feitelson MA, and Jay G (1995). Functional inactivation but not structural mutation of *p53* causes liver cancer. *Nat Genet* **9**, 41–47.

[18] Hohne M, Schaefer S, Seifer M, Feitelson MA, Paul D, and Gerlich WH (1990). Malignant transformation of immortalized transgenic hepatocytes after transfection with hepatitis B virus DNA. *EMBO J* **9**, 1137–45.

[19] Luber B, Arnold N, Sturzl M, Hohne M, Schirmacher P, Lauer U, Wienberg J, Hofschneider PH, and Kekule AS (1996). Hepatoma-derived integrated HBV DNA causes multi-stage transformation *in vitro*. *Oncogene* **12**, 1597–608.

[20] Rossner MT (1992). Hepatitis B virus X-gene product: a promiscuous transcriptional activator. *J Med Virol* **36**, 101–17.

[21] Benn J, and Schneider RJ (1994). HBV X protein activates ras–GTP complex formation and establishes a ras, raf, MAP kinase signaling cascade. *Proc Natl Acad Sci USA* **91**, 10350–54.

[22] Lucito R, and Schneider RJ (1992). Hepatitis B virus protein activates transcription factor NF-κB without a requirement for protein kinase C. *JVirol* **66**, 983–91.

[23] Natoli G, Avantaggiati ML, Chirillo P, Costanzo A, Artini M, Balsano C, and Levrero M (1994). Induction of the DNA binding activity of c-Jun/c-Fos heterodimers by the hepatitis B virus transactivator pX. *Mol Cell Biol* **14**, 989–98.

[24] Lee YH, and Yun Y (1998). HBx protein of hepatitis B virus activates Jak1-STAT signaling. *J Biol Chem* **273**, 25510–15.

[25] Cheong JH, Yi M, Lin Y, and Murakami S (1995). Human RPB5, a subunit shared by eukaryotic nuclear RNA polymerases, binds human hepatitis B virus X protein and may play a role in X transactivation. *EMBO J* **14**, 142–50.

[26] Qadri K, Maguire HF, and Siddiqui A (1995). Hepatitis B virus *trans*-activator protein X interacts with the TATA-binding protein. *Proc Natl Acad Sci USA* **92**, 1003–1007.

[27] Maguire HF, Hoeffler JP, and Siddiqui A (1991). HBV X protein alters the DNA binding specificity of CREB and ATF-2 by protein–protein interactions. *Science* **252**, 842–44.

[28] Haviv I, Vaizel D, and Shaul Y (1995). The X protein of hepatitis B virus coactivates potent activation domains. *Mol Cell Biol* **15**, 1079–85.

[29] Haviv I, Vaizel D, and Shaul Y (1996). pX, the HBV-encoded coactivator, interacts with components of the transcription machinery and stimulates transcription in a TAF-independent manner. *EMBO J* **15**, 3413–20.

[30] Lee TH, Elledge SJ, and Butel JS (1995). Hepatitis B virus X protein interacts with a probable cellular DNA repair protein. *J Virol* **69**, 1107–14.

[31] Wang XW, Forrester K, Yeh H, Feitelson MA, Gu J, and Harris CC (1994). Hepatitis B virus X protein inhibits p53 sequence-specific DNA binding, transcriptional activity and association with ERCC3. *Proc Natl Acad Sci USA* **91**, 2230–34.

[32] Feitelson MA, Zhu M, Duan LX, and London WT (1993). Hepatitis B x antigen and p53 are associated *in vitro* and in liver tissues from patients with primary hepatocellular carcinoma. *Oncogene* **8**, 1109–17.

[33] Sun BS, Zhu X, Clayton MM, Pan J, and Feitelson MA (1998). Identification and preliminary characterization of a protein involved in cellular senescence which binds to hepatitis B virus X antigen. *Hepatology* **27**, 228–39.

[34] Feitelson MA, Reis H, Pan J, Lian Z, Fang J, Liu J, Zhu X, Zhu M, and Sun B (1999). Abrogation of negative growth regulatory pathways by hepatitis B virus encoded X antigen in the development of hepatocellular carcinoma. In *Normal and Malignant Liver Cell Growth: FALK Workshop*. WE Fleig (Ed). Kluwer Academic Publishers, Lancaster, UK. pp. 156–70.

[35] Lian Z, Pan J, Liu J, Zhu M, Arbuthnot P, Kew MC, and Feitelson MA (1999). The translation initiation factor, SUI1, may be a target of hepatitis B x antigen in hepatocarcinogenesis. *Oncogene* **18**, 1677–87.

[36] Elmore LW, Hancock AR, Chang SF, Wang XW, Chang S, Callahan CP, Geller DA, Will H, and Harris CC (1997). Hepatitis B virus X protein and p53 tumor suppressor interactions in the modulation of apoptosis. *Proc Natl Acad Sci USA* **94**, 14707–12.

[37] Kim H, Lee H, and Yun Y (1998). X-gene product of hepatitis B virus induces apoptosis in liver cells. *J Biol Chem* **273**, 381–85.

[38] Sirma H, Giannini C, Poussin K, Paterlini P, Kremsforf D, and Brechot C (1999). Genetic and functional analysis of the effects of hepatitis B viral transactivator HBx on cell growth and apoptosis: implications for viral replication and hepatocarcinogenesis. In *Normal and Malignant Liver Cell Growth: FALK Workshop*. WE Fleig (Ed). Kluwer Academic Publishers, Lancaster, UK. pp. 171–86.

[39] Gottlob K, Fulco M, Levrero M, and Graessmann A (1998). The hepatitis B virus HBx protein inhibits caspase 3 activity. *J Biol Chem* **273**, 33347–53.

[40] Benn J, and Schneider RJ (1995). Hepatitis B virus HBx protein deregulates cell cycle checkpoint controls. *Proc Natl Acad Sci USA* **92**, 11215–19.

[41] Kim SO, Park JG, and Lee YI (1996). Increased expression of the insulin-like growth factor I (IGF-I) receptor gene in hepatocellular carcinoma cell lines: implications of IGF-I receptor gene activation by hepatitis B virus X gene product. *Cancer Res* **56**, 3831–36.

[42] Su Q, Liu JF, Zhang SX, Li DF, and Yang JJ (1994). Expression of insulin-like growth factor II in hepatitis B, cirrhosis and hepatocellular carcinoma: its relationship with hepatitis B virus antigen expression. *Hepatology* **19**, 788–99.

[43] Ohmachi YA, Murata T, Yasuda K, Kitagawa S, Yamamoto M, Monden T, Mori N, Matsuura K, and Matsubara K (1994). Expression of the pancreatic secretory trypsin inhibitor gene in the liver infected with hepatitis B virus. *J Hepatol* **21**, 1012–16.

[44] Zhou MX, Watabe, M, and Watabe K (1994). The X-gene of human hepatitis B virus transactivates the c-*jun* and alpha-fetoprotein genes. *Arch Virol* **134**, 369–78.

[45] Aden DP, Fogel A, Plotkin, S, Damjanov I, and Knowles BB (1979). Controlled synthesis of HBxAg in a differentiated human liver carcinoma-derived cell line. *Nature* **282**, 615-16.

[46] Sells MA, Chen ML, and Acs G (1987). Production of hepatitis B virus particles in Hep G2 cells transfected with cloned hepatitis B virus DNA. *Proc Natl Acad Sci USA* **84**, 1005–1009.

[47] Danos O (1991). Viral vectors for gene expression. In *Methods in Molecular Biology, Practical Molecular Virology*. M Collins (Ed). Humana Press, Clifton, NJ. pp. 17–27.

[48] Lian Z, Liu J, Pan J, Tufan NLS, Zhu M, Arbuthnot P, Kew M, Clayton MM, and Feitelson MA (2001). A cellular gene up-regulated by hepatitis B virus encoded X antigen promotes hepatocellular growth and survival. *Hepatology* **34**, 146–57.

[49] Duan LX, Zhu MH, Bagasra O, and Pomerantz RJ (1995). Intracellular immunization against HIV-1 infection of human T lymphocytes: utility of anti-Rev single-chain variable fragments. *Hum Gene Ther* **6**, 1561–73.

[50] Benson DA, Boguski MS, Lipman DJ, and Ostell J (1997). GenBank. *Nucleic Acids Res* **25**, 1–6.

[51] Feitelson MA, Millman I, Duncan GD, and Blumberg BS (1988). Presence of antibodies to the polymerase gene product(s) of hepatitis B and woodchuck hepatitis virus in natural and experimental infections. *J Med Virol* **24**, 121–36.

[52] Ozoren NEDW (2000). Introduction to cancer genes and growth control. In *DNA Alterations in Cancer, Genetic and Epigenetic Changes*. M Ehrlich (Ed). Eaton Publishing, Natick, MA. pp. 3–43.

[53] Shin SI, Freedman VH, Risser R, and Pollack R (1975). Tumorigenicity of virus-transformed cells in nude mice is correlated specifically with anchorage independent growth *in vitro*. *Proc Natl Acad Sci USA* **72**, 4435–39.